

CHORUS

This is the accepted manuscript made available via CHORUS. The article has been published as:

Charge-exchange x-ray spectra: Evidence for significant contributions from radiative decays of doubly excited states

R. Ali, P. Beiersdorfer, C. L. Harris, and P. A. Neill

Phys. Rev. A **93**, 012711 — Published 21 January 2016

DOI: [10.1103/PhysRevA.93.012711](https://doi.org/10.1103/PhysRevA.93.012711)

Charge-exchange x-ray spectra: Evidence for significant contributions from radiative decays of doubly excited states

R. Ali,¹ P. Beiersdorfer,² C. L. Harris,³ and P. A. Neill⁴

¹*Department of Physics, The University of Jordan, Amman 11942, Jordan; ramimali@ju.edu.jo*

²*Lawrence Livermore National Laboratory, Livermore, CA 94550-9234, USA; beiersdorfer1@llnl.gov*

³*Natural Sciences Division, Gulf Coast State College,*

Panama City, FL 32401, USA; charris@gulfcoast.edu

⁴*Department of Physics, University of Nevada, Reno, NV 89557, USA; paul@unr.edu*

Charge exchange collisions of slow Ne^{10+} ions with He, Ne, and Ar targets were studied with simultaneous x-ray and cold-target recoil-ion momentum spectroscopy proving the contribution of several mechanisms to the radiative stabilization of apparent (4,4) doubly excited states for He and Ne targets and of (5,6) states for Ar. In particular, the stabilization efficiency of the dynamic auto-transfer to Rydberg states mechanism is confirmed. Moreover, we present evidence for direct radiative decays of (4,4) states populated in collisions with He, which may be the first experimental indication of the population of so-called unnatural parity states in such collisions. These mechanisms lead to the emission of x rays that have considerably higher energies than those predicted by current spectral models and may explain recent observations of anomalously large x-ray emission from Rydberg levels.

PACS numbers: 34.70.+e, 32.30.Rj, 32.80.Ee, 32.80.Zb

I. INTRODUCTION

K-shell x-ray spectroscopy has become the primary tool for diagnosing electron capture, or charge exchange, in slow collisions of highly charged ions with atoms and molecules in astronomical environments, such as planetary atmospheres, cometary comae, stellar nurseries, and the heliosphere [1–6]; largely because charge exchange produces specific signatures in the x-ray emission not seen in spectra formed by electron-impact. While the predicted emission in fast collisions with atomic hydrogen appears to match observations [7], this is not the case in slow collisions with molecules and multi-electron atoms, even with H₂ and He. Laboratory measurements, especially those from ion traps, have yielded x-ray spectra whose detailed spectral intensities are at odds with spectral models [8–12].

Many of the discrepancies have been tied to the fact that more than one electron may be captured from multi-electron targets [13–15]. Indeed, early spectral models [16, 17] have neglected multi-electron capture; an issue later called into question [18, 19]. Somewhat improved predictions were obtained by more recent models that included some multi-electron capture features [20–22]. These models, however, assumed that electrons captured into multiply excited states undergo one or more autoionization processes before the remaining electron, or two electrons if too far away from each other to make autoionization efficient, de-excites by x-ray emission; an assumption that does not explain the anomalously large x-ray emission from Rydberg levels that has been puzzling since its first observation [8]. In particular, these models assume that true double electron capture processes, in which only two electrons are initially captured and both stabilize radiatively, do not occur or that their occurrence is negligibly small. In order to avoid possibly erroneous conclusions that may result from this assumption and to better interpret and predict charge-exchange produced x-ray spectra, the population and deexcitation pathways of multiply excited states must be understood. Multi-electron capture can involve far more than two electrons; however, before a full model that includes all possible deexcitation pathways of multiply excited states can be developed, it is necessary to first understand the role of double electron capture, as it is the most probable multi-electron capture process.

Predictions of classical overbarrier models [23, 24] on multi-electron capture were generally found in fair agreement with experiment [13, 14, 25–30]. They predict double capture to populate symmetric ($n = n'$) or quasi-symmetric ($n \approx n'$) doubly excited states; widely believed to dominantly autoionize. However, unexpectedly high radiative stabilization probabilities, P_{rad} , of both electrons

$$P_{rad} = \sigma_{TDC} / (\sigma_{TDC} + \sigma_{ADC}) \quad (1)$$

were reported [31–35], where σ_{TDC} and σ_{ADC} are the cross sections for radiatively stabilized or true double capture (TDC) and autoionizing double capture (ADC), respectively. Various mechanisms for populating asymmetric Rydberg states ($n \ll n'$), believed to have large fluorescence yields, were proposed. Photon emission from Rydberg transitions following multi-electron capture [36] and energy gain measurements [37] lent support to this conjecture. These mechanisms include the 2-step uncorrelated double capture followed by post-collisional auto-transfer to Rydberg states [38–40] feeding ($n \ll n'$) from ($n = n'$) or ($n \approx n'$) states, the 1-step correlated double capture [41], the 2-step correlated transfer excitation [42], and 2-step transfer excitation involving nucleus-electron interaction [43]. The population of certain intershell ($n \neq n'$) states [44] and some symmetric ($n = n'$) singlet states with “unnatural” parity $\pi = (-1)^{L+1}$ [45–47] that have high fluorescence yields was also suggested. It was argued, however, that these states have low statistical weight and no strong evidence of their population existed [34, 48], but that high resolution spectroscopy in the soft x-ray range could directly identify the relevant states if populated [48].

Ne¹⁰⁺+He is a collision system that received much attention, but without reaching consensus. Several experimental reports argued in favor of correlated double capture and correlated transfer excitation [49–51], while others stressed the importance of auto-transfer to Rydberg states [43, 52–55]; whereas a theoretical study [56] found that both auto-transfer to Rydberg states and static configuration interaction populate the (3, *n*) Rydberg series. The debate continued in more recent work involving other collision systems [57, 58]. In the following, we presents a highly differential study of autoionizing double capture and true double capture utilizing simultaneous x-ray and cold target recoil ion momentum spectroscopy, reminiscent of the pioneering work utilizing simultaneous x-ray and energy gain spectroscopy [59–61], to study 100 keV Ne¹⁰⁺ with He, Ne, and Ar collisions. This combination provides subpartial x-ray spectra originating in (*n*, *n'*) states enabling unprecedented scrutiny of their population and deexcitation pathways.

II. EXPERIMENT

Figure 1 shows a schematic of the experimental setup which has been described in detail in [62]. Briefly, ²²Ne¹⁰⁺ ions from the University of Nevada, Reno, electron cyclotron resonance ion source crossed supersonic target jets. Electric fields guided recoil ions onto a position-sensitive detector and charge analyzed projectile ions that were then detected by another position-sensitive detector. The impact position provided the final projectile charge state, while

time-of-flight and impact position provided the recoil ion charge state, the scattering angle θ and the collision Q -value [63], i.e., the change in the system electronic energy which defines its quantum state after the collision. The detection of a doubly charged target ion (He^{2+} , Ne^{2+} , Ar^{2+}) in coincidence with a Ne^{9+} projectile ion defines an autoionizing double capture event, and with Ne^{8+} a true double capture event. X-rays emitted at 90° to the incident ions were detected by a windowless detector. The full-width-at-half-maximum of x-ray lines is energy-dependent and was 126 and 133 eV for the Ne^{9+} Ly α and Ly δ lines, respectively.

FIG. 1. (Color online) Schematic of the experimental setup.

III. RESULTS AND DISCUSSION

The recoil ion momentum spectroscopy results are shown in Fig. 2. It is evident from the figure that the collision systems we studied have a high radiative stabilization probability, and that the assumption in current x-ray models that $P_{rad} = 0$ is violated in a significant way. Indeed, the overall P_{rad} is $(31.9 \pm 0.8)\%$, $(11.4 \pm 0.2)\%$, and $(21.2 \pm 0.1)\%$ for the He, Ne, and Ar targets, respectively. Moreover, it is readily seen that true double capture for all three targets is dominated by narrow Q -value ranges associated with $(n = n')$ or $(n \approx n')$ states that are quasi-degenerate with $(n \ll n')$ ones. For events falling within the Q -value region of interest for each target, appreciably larger configuration specific $P_{rad}^{(n,n')}$ are obtained. Specifically, $P_{rad}^{(4,4)+(3,n \geq 9)} = (44.9 \pm 1.4)\%$ for He and $(33.4 \pm 0.6)\%$ for Ne, while $P_{rad}^{(5,6)+(4,n \geq 15)} = (33.6 \pm 0.6)\%$ for Ar.

FIG. 2. (Color online) Density plots for the scattering angle θ versus Q -value for autoionizing double capture (top row) and true double capture (middle row) in collisions of 100 keV $^{22}\text{Ne}^{10+}$ with He (left column), Ne (middle column), and Ar (right column) targets. Plots are on the same scale for each target. The bottom row displays the projected autoionizing double capture (\bullet) and true double capture (\blacktriangle) Q -value spectra corrected for double collisions (2.6% for He, 1.8% for Ne, 4.6% for Ar) and for random coincidences. The two dotted vertical lines for each target define the Q -value region of interest where a high P_{rad} is observed. Q -value ranges corresponding to specific (n, n') states, as calculated with the Hartree-Fock atomic structure code by Cowan [64], are indicated by vertical square brackets, while the (n, ∞) series limits are indicated by vertical solid lines. The insets compare the normalized autoionizing double capture (\bullet) and true double capture (\blacktriangle) angular distributions for events within each target region of interest. Classical scattering angles corresponding to 1-step correlated double capture (\circ), 2-step uncorrelated double capture (\square), and 2-step correlated transfer excitation and/or 2-step transfer excitation involving nucleus-electron interaction (\diamond) are indicated.

The x-ray spectra originating in double electron capture are displayed in Fig. 3. All spectra have been corrected for double collisions but not for the random coincidences in the triple-coincidence measurements, because these are essentially negligible due to the very low count rate of x-rays (which was less than 2 counts/s). The top row shows overlays of the partial x-ray spectra from autoionizing double capture and true double capture. $K_{\alpha,\beta,\dots}(n')$ designate $(np, n'l') \rightarrow (1s, n'l')$ x-rays, while $K_{\alpha,\beta,\gamma,\dots}$ denote $(1s, np) \rightarrow (1s^2)$ x-rays. We used the same Ly α, β, \dots line energies for the $K_{\alpha,\beta,\dots}(n')$ lines due to their very close energies. For example, the mid-energy point for $K_\gamma(n' = 4)$ x-rays is 1276 eV compared to 1277 eV for Ly γ . Using Ly β line energy for $K_\beta(n' \geq 9)$, Ly γ for $K_\gamma(n' \geq 15)$, or Ly α for $K_\alpha(n'_{large})$ is also justified since the Rydberg electron is a distant spectator.

FIG. 3. (Color online) Partial autoionizing double capture and true double capture x-ray spectra (top row) and subpartial x-ray spectra corresponding to each target region of interest defined in Fig. 2 (lower three rows) in collisions of 100 keV $^{22}\text{Ne}^{10+}$ with He (left column), Ne (middle column), and Ar (right column) targets. Error bars represent statistical and double collision correction uncertainties added in quadrature. Locations of the H-like Ne^{9+} Ly α, β, \dots , and He-like Ne^{8+} K_α, K_γ , and $K_{\alpha,\beta,\dots}(n')$ lines are indicated. Fitting results for the subpartial spectra are shown in the lower two rows. Numbers represent percentage peak areas and corresponding uncertainties.

The figure clearly shows that the detected true double capture x-ray intensity is not negligible. True double capture accounts for $(40.7 \pm 2.5)\%$, $(20.0 \pm 1.0)\%$, and $(24.2 \pm 1.2)\%$ of the total double capture x-ray intensity for He, Ne, and Ar, respectively. The true double capture x-ray intensity is even larger for the states (n, n') in the regions of interest of Fig. 2, whose subpartial x-ray spectra are displayed in the second row of Fig. 3, accounting for $(53.3 \pm 3.2)\%$, $(47.5 \pm 2.8)\%$, and $(31.5 \pm 2.0)\%$ for He, Ne, and Ar, respectively. Undoubtedly, spectral models that assume multi-electron capture is followed only by autoionization are bound to yield erroneous conclusions.

Figure 3 also shows that all autoionizing double capture partial spectra are dominated by $\text{Ly}\alpha$. This is expected as they result from lower-lying singly excited states created by autoionization. By contrast, the combined K_α and $K_\alpha(n')$ lines of the true double capture partial spectra are comparable to the higher energy ones.

In order to identify the mechanisms underlying the high values of P_{rad} , we need to perform an analysis of the angular distributions shown in the insets of Fig. 2 as well as of the subpartial x-ray spectra shown in the last two rows of Fig. 3. The insets of Fig. 2 compare normalized autoionizing double capture and true double capture angular distributions for events within each target region of interest, and reveal a double-peaked distribution for He but broad structures for Ne and Ar. Following Refs. [43, 65], classical scattering angles for the different mechanisms were computed using Coulomb potential energy curves and classical trajectories for configurations within each target region of interest, and indicated on Fig. 2. For the 2-step correlated transfer excitation and/or 2-step transfer excitation involving nucleus-electron interaction we have used the dominant single electron capture channels, $n = 5$ for He and Ne and $n = 6$ for Ar [12], as promoters to the final double capture channels. The uncorrelated and correlated double capture angles for all targets lie in the vicinity of angular distributions maxima, but their relative importance cannot be judged from the distributions alone. By contrast, the 2-step correlated and/or 2-step transfer excitation involving nucleus-electron interaction scattering angle for He clearly corresponds to the second peak in both autoionizing double capture and true double capture angular distributions, indicating these mechanisms contribute to double capture from He.

The last two rows of Fig. 3 show Gaussian fits for the autoionizing double capture and true double capture subpartial spectra. The $\text{Ly}\beta$ lines in both He and Ne autoionizing double capture spectra represent direct experimental evidence that the symmetric $(4, 4)$ $1S^e(4)$ state, which is the only state among the $\text{Ne}^{8+}(4, 4)$ singlet and triplet terms above the $(3, \infty)$ limits [47, 66], has been populated and subsequently autoionized to $3p$. Similarly, the Ar autoionizing double capture subpartial spectrum exhibits a small $\text{Ly}\gamma$ line due to population of $4p$ by autoionization of the quasi-symmetric $(5, 6)$ states above the $(4, \infty)$ limits.

Another observation of particular importance to the present study is that the fit of the true double capture subpartial spectrum of He shows that the spectrum exhibits a $K_\gamma(n' = 4)$ line from direct $(4p, 4l') \rightarrow (1s, 4l')$ transitions. This line accounts for $(19.0 \pm 4.7)\%$ of the counts in the spectrum, with a negligible contribution from random coincidences to the uncertainty, and corresponds to $\approx 10\%$ of the total autoionizing double capture and true double capture x rays originating in the $(4, 4)$ and $(3, n \geq 9)$ states. This is in the neighborhood of what one expects from the low statistical weight of the symmetric $(4l, 4l')$ unnatural parity terms which number only 4 out of the 24 singlet terms [47], but which have significant fluorescence yields [45–47]. This observation may represent the first experimental suggestion that these unnatural parity states are populated in such collisions.

From the He data shown in Figs. 2 and 3 we can, thus, conclude that 2-step uncorrelated double capture populating symmetric $(4, 4)$ states, 2-step uncorrelated double capture followed by auto-transfer to Rydberg states, 1-step correlated double capture, and 2-step correlated and/or 2-step transfer excitation involving nucleus-electron interaction coexist and altogether contribute to P_{rad} .

Support for the auto-transfer to Rydberg states mechanism is given by the Ne target data, which unlike the He data, exhibits an absence of the $K_\gamma(n' = 4)$ in the true double capture subpartial spectrum. Since population of the $(4, 4)$ $1S^e(4)$ state, thus other $(4l, 4l')$ states, has been confirmed by the Ne autoionizing double capture subpartial spectrum, this absence rules out contribution by direct radiative stabilization to true double capture from Ne. Since also the $n = 4$ Ne^{9+} x-ray spectra following single electron capture by 100 keV Ne^{10+} from both He and Ne [12] exhibited strong $\text{Ly}\gamma$ lines implying significant $4p$ population, it is unlikely that uncorrelated double capture populates $(4p, 4l')$ for He but not for Ne. This absence, however, is consistent with the radiative decays and cascades of $(3, n'_{large})$ supporting the auto-transfer to Rydberg states of $(4, 4)$ to $(3, n'_{large})$ states.

Another observation that supports the auto-transfer to Rydberg states mechanism is the absence of the $2^3P_1 \rightarrow 1^1S_0$ intercombination line from the Ne true double capture spectrum. The fitting procedure is capable of deconvoluting this line from the $2^1P_1 \rightarrow 1^1S_0$ line [67], and, if present, the line would be detectable. Given that, contrary to He, triplet states are populated in double capture from Ne [25], most of the triplet-triplet cascade transitions feeding 2^3P_1 from initial $(4, 4)^3L$ states, and the final $2^3P_1 \rightarrow 1^1S_0$ are fast and should take place in view of the x-ray detector. Given also the findings of higher fluorescence yields for triplet $(4l, 4l')$ states than for singlets in neighboring O^{6+} [46], the absence implies 2^3P_1 states are not fed in view of the detector although Ne^{8+} ions spend about 4 ns there. This is possible for Rydberg electrons with large enough nl values that undergo slow transitions down the Yrast chain $(n, l = n - 1) \rightarrow (n - 1, l = n - 2)$. The absence of the intercombination line, thus, also supports the auto-transfer to Rydberg states mechanism.

Although $(4, 4)$ and $(3, n \geq 9)$ states are populated in double capture from Ne as from He, the absence of a 2-step correlated and/or 2-step transfer excitation involving nucleus-electron interaction angular distribution peak for the Ne target in Fig. 2 rules out these mechanisms as population mechanisms of $(3l, n'l')$ states, but the 1-step correlated double capture process remains possible. Nevertheless, since uncorrelated double capture has been confirmed to populate $(4l, 4l')$, and given the similarity of the autoionizing double capture and true double capture angular distributions for the assumed $(4, 4)$ and $(3, n \geq 9)$ states implying the same primary population mechanism

for both, and the absence of $K_\gamma(n' = 4)$ and the $2^3P_1 \rightarrow 1^1S_0$ lines from the true double capture subpartial spectrum, the present study of $\text{Ne}^{10+} + \text{Ne}$ collisions has furnished collective evidence for the high efficiency of the refined auto-transfer to Rydberg states mechanism [40] in transferring (4, 4) states populated by uncorrelated double capture into (3, $n \geq 9$).

The Ar true double capture subpartial x-ray spectrum exhibits similar features to that of Ne where the $2^3P_1 \rightarrow 1^1S_0$, $K_\delta(n' = 6)$, and $K_\epsilon(n' = 5)$ lines are absent, which is consistent with the population of (4, n'_{large}) states. The same logic developed for Ne applies to Ar, with the conclusion that the auto-transfer to Rydberg states mechanism is highly efficient in transferring (5, 6) states into (4, $n \geq 15$).

IV. CONCLUSIONS

In conclusion, this work provides evidence that double electron capture leads to significant x-ray production in ways not yet included in spectral models, even in those that already include multi-electron capture, namely, direct radiative stabilization and auto-transfer to Rydberg states. There is no (simple) way yet to know *a priori* whether both mechanisms contribute in an arbitrary collision system, but both result in x-ray energies that are significantly higher than possible through autoionization.

The observation of direct radiative decays of (4,4) doubly excited states populated in Ne^{10+} on He collisions may represent the first experimental suggestion that unnatural parity doubly excited states are populated in such collisions. The fact that double capture may stabilize radiatively, i.e., without autoionization, may explain the puzzling intensity of the $9p \rightarrow 1s$ Lyman line observed in $\text{P}^{15+} + \text{H}_2$ collisions [11]. It is possible that this high-energy line contains contributions from direct radiative decays of P^{13+} (9p, 9l') states, as the energies are indistinguishable even with high-resolution x-ray microcalorimeters [11]. This means that the enhancement of H-like Rydberg lines may actually be from He-like ions produced by double capture and mimicking Lyman series x rays while undergoing direct radiative deexcitation.

ACKNOWLEDGMENTS

Work at the Lawrence Livermore National Laboratory was performed under the auspices of the U.S. Department of Energy under Contract DE-AC52-07NA27344 and supported in part by NASA's Astrophysics Research and Analysis program.

-
- [1] T. E. Cravens, *Geophys. Res. Lett.* **24**, 105 (1997).
 - [2] C. M. Lisse *et al.*, *Science* **292**, 1342 (2001).
 - [3] R. Pepino *et al.*, *Astrophys. J.* **617**, 1347 (2004).
 - [4] K. Dennerl *et al.*, *Astron. Astrophys.* **451**, 709 (2006).
 - [5] T. Montmerle and L. K. Townsley, *Astron. Nachrichten* **333**, 355 (2012).
 - [6] Q. D. Wang and J. Liu, *Astron. Nachrichten* **333**, 373 (2012).
 - [7] P. Beiersdorfer, M. Bitter, M. Marion, and R. E. Olson, *Phys. Rev. A* **72**, 032725 (2005).
 - [8] P. Beiersdorfer *et al.*, *Phys. Rev. Lett.* **85**, 5090 (2000).
 - [9] P. Beiersdorfer *et al.*, *Science* **300**, 1558 (2003).
 - [10] F. I. Allen *et al.*, *Phys. Rev. A* **78**, 032705 (2008).
 - [11] M. A. Leutenegger, P. Beiersdorfer, G. V. Brown, R. L. Kelley, C. A. Kilbourne, and F. S. Porter, *Phys. Rev. Lett.* **105**, 063201 (2010).
 - [12] R. Ali *et al.*, *Astrophys. J. Lett.* **716**, L95 (2010).
 - [13] M. Barat and P. Roncin, *J. Phys. B* **25**, 2205 (1992).
 - [14] R. Ali *et al.*, *Phys. Rev. A* **49**, 3586 (1994).
 - [15] M. Trassinelli *et al.*, *J. Phys. B* **45**, 085202 (2012).
 - [16] R. M. Häberli *et al.*, *Science* **276**, 939 (1997).
 - [17] V. Kharchenko *et al.*, *Astrophys. J.* **585**, L73, (2003).
 - [18] A. A. Hasan *et al.*, *Astrophys. J.* **560**, L205 (2001).
 - [19] R. Ali *et al.*, *Astrophys. J.* **629**, L125 (2005).
 - [20] A. Salehzadeh and T. Kirchner, *J. Phys. B* **46**, 025201 (2013).
 - [21] L. Liu, J. G. Wang, and R. K. Janev, *Phys. Rev. A* **89**, 012710 (2014).
 - [22] S. Otranto, N. D. Cariatore, and R. E. Olson, *Phys. Rev. A* **90**, 062708 (2014).
 - [23] A. Bárány *et al.*, *Nucl. Instrum. Methods B* **9**, 397 (1985).

- [24] A. Niehaus, *J. Phys. B* **19**, 2925 (1986).
- [25] P. Benoit-Cattin *et al.*, *J. Phys. B* **21**, 3387 (1988).
- [26] J. H. Posthumus and R. Morgenstern, *Phys. Rev. Lett.* **68**, 1315 (1992).
- [27] G. de Nijs, R. Hoekstra, and R. Morgenstern, *J. Phys. B* **29**, 6143 (1996).
- [28] H. Merabet *et al.*, *Phys. Rev. A* **59**, R3158 (1999).
- [29] E. D. Emmons, A. A. Hasan, and R. Ali, *Phys. Rev. A* **60**, 4616 (1999).
- [30] A. A. Hasan *et al.*, *Phys. Rev. Lett.* **83**, 4522 (1999).
- [31] P. Roncin, M. N. Gaboriaud, and M. Barat, *Europhys. Lett.* **16**, 551 (1991).
- [32] H. Cederquist *et al.*, *Phys. Rev. A* **46**, 2592 (1992).
- [33] R. Ali *et al.*, *J. Phys. B* **26**, L177 (1993).
- [34] M. N. Gaboriaud, P. Roncin, and M. Barat, *J. Phys. B* **26**, L303 (1993).
- [35] S. Martin *et al.*, *Phys. Rev. A* **48**, 1171 (1993).
- [36] S. Martin *et al.*, *Phys. Rev. A* **42**, 6564 (1990).
- [37] H. Cederquist, C. Biedermann, N. Selberg, and P. Hvelplund, *Phys. Rev. A* **51**, 2169 (1995).
- [38] H. Bachau, P. Roncin, and C. Harel, *J. Phys. B* **25**, L109 (1992).
- [39] P. Roncin *et al.*, *J. Phys. B* **26**, 4181 (1993).
- [40] A. K. Kazansky and P. Roncin, *J. Phys. B* **27**, 5537 (1994).
- [41] N. Stolterfoht *et al.*, *Phys. Rev. Lett.* **57**, 74 (1986).
- [42] H. Winter *et al.*, *Phys. Rev. Lett.* **58**, 957 (1987).
- [43] X. Flechard *et al.*, *J. Phys. B* **30**, 3697 (1997).
- [44] Z. Chen and C. D. Lin, *J. Phys. B* **26**, 957 (1993).
- [45] N. Vaeck and J. E. Hansen, *J. Phys. B* **26**, 2977 (1993).
- [46] H. W. van der Hart, N. Vaeck, and J. E. Hansen, *J. Phys. B* **27**, 3489 (1994).
- [47] H. W. van der Hart, N. Vaeck, and J. E. Hansen, *J. Phys. B* **28**, 5207 (1995).
- [48] P. Roncin, M. N. Gaboriaud, Z. Szilagyi, and M. Barat, in *Proceedings of the XVIIIth International Conference on the Physics of Electronic and Atomic Collisions*, edited by T. Andersen, B. Fastrup, F. Folkmann, H. Knudsen, and N. Andersen, AIP Conf. Proc. **295** (AIP, New York, 1993), p537.
- [49] F. Fremont, H. Merabet, J. -Y. Chesnel, X. Husson, A. Lepoutre, D. Lecler, G. Rieger, and N. Stolterfoht, *Phys. Rev. A* **50**, 3117 (1994).
- [50] J. -Y. Chesnel *et al.*, *Phys. Rev. A* **53**, 4198 (1996).
- [51] J. -Y. Chesnel, H. Merabet, B. Sulik, F. Fremont, C. Bedouet, X. Husson, M. Grether, and N. Stolterfoht, *Phys. Rev. A* **58**, 2935 (1998).
- [52] A. Bordenave-Montesquieu, P. Moretto-Capelle, A. Gonzalez, M. Benhenni, H. Bachau, and I. Sánchez, *J. Phys. B* **27**, 4243 (1994).
- [53] S. Martin *et al.*, *Phys. Rev. A* **52**, 1218 (1995).
- [54] P. Roncin and M. Barat, *Phys. Scr. T* **73**, 188 (1997).
- [55] X. Flécharde *et al.*, *J. Phys. B* **34**, 2759 (2001).
- [56] I. Sánchez and H. Bachau, *J. Phys. B* **28**, 795 (1995).
- [57] W. Chen *et al.*, *Phys. Rev. A* **88**, 052703 (2013).
- [58] Y. Xue *et al.*, *Phys. Rev. A* **90**, 052720 (2014).
- [59] J. P. Rozet *et al.*, *Nucl. Instrum. Methods A* **262**, 84 (1987).
- [60] A. Touati *et al.*, *Nucl. Instrum. Methods B* **23**, 64 (1987).
- [61] A. Chetioui *et al.*, *J. Phys. B* **23**, 3659 (1990).
- [62] R. Ali, in *Proceedings of the 15th International Conference on Atomic Processes in Plasmas*, edited by J. D. Gillaspay, J. J. Curry, and W. L. Wiese, AIP Conf. Proc. **926** (AIP, 2007), p. 216.
- [63] R. Ali *et al.*, *Phys. Rev. Lett.* **69**, 2491 (1992).
- [64] R. D. Cowan, *The Theory of Atomic Structure and Spectra* (University of California Press, Berkeley, CA, 1981).
- [65] M. A. Abdallah *et al.*, *Phys. Rev. A* **57**, 4373 (1998).
- [66] Y. K. Ho, *Phys. Lett.* **79A**, 44 (1980).
- [67] F. Eissa, Ph.D. Dissertation, University of Nevada, Reno, 2007.

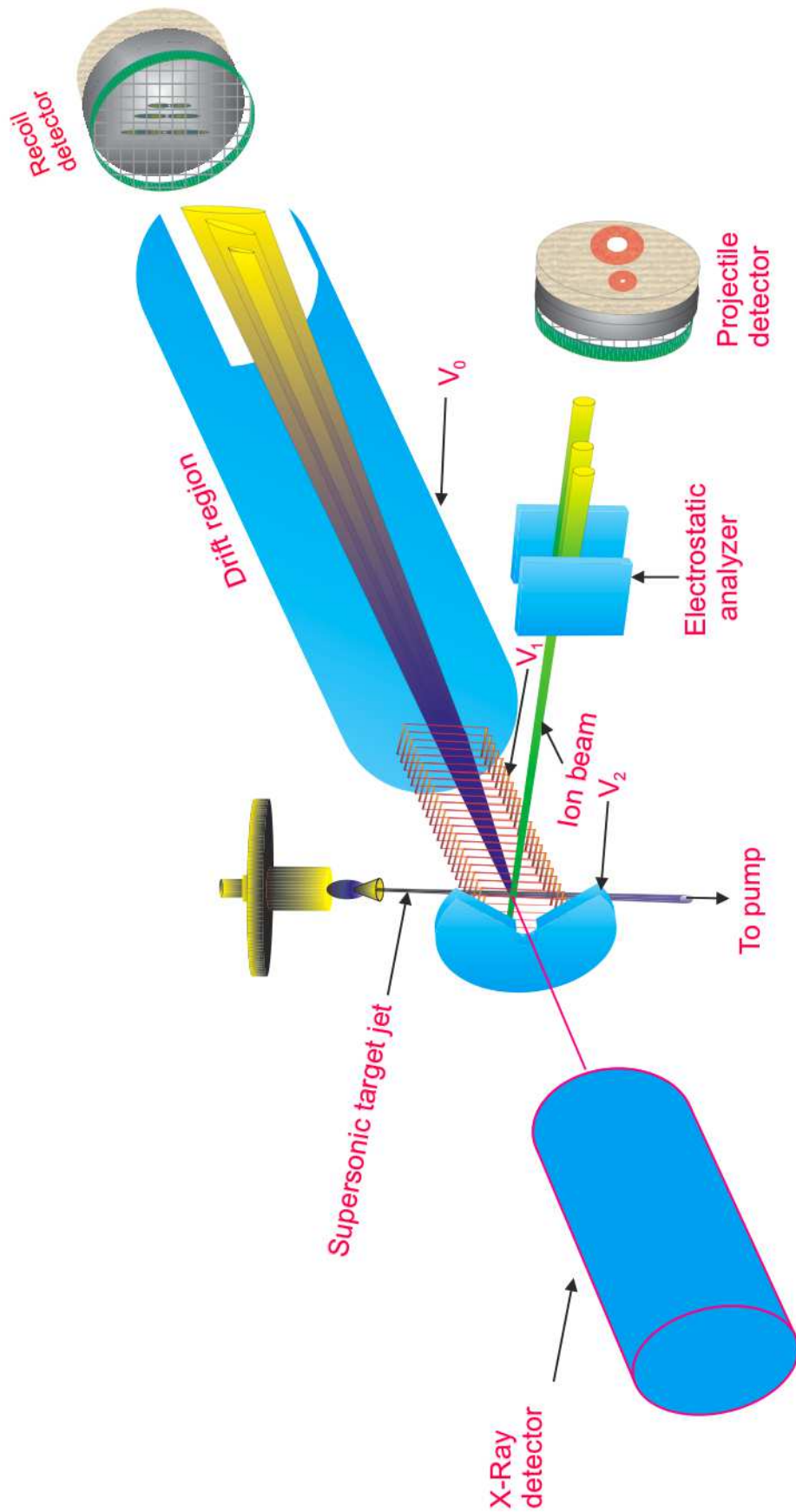
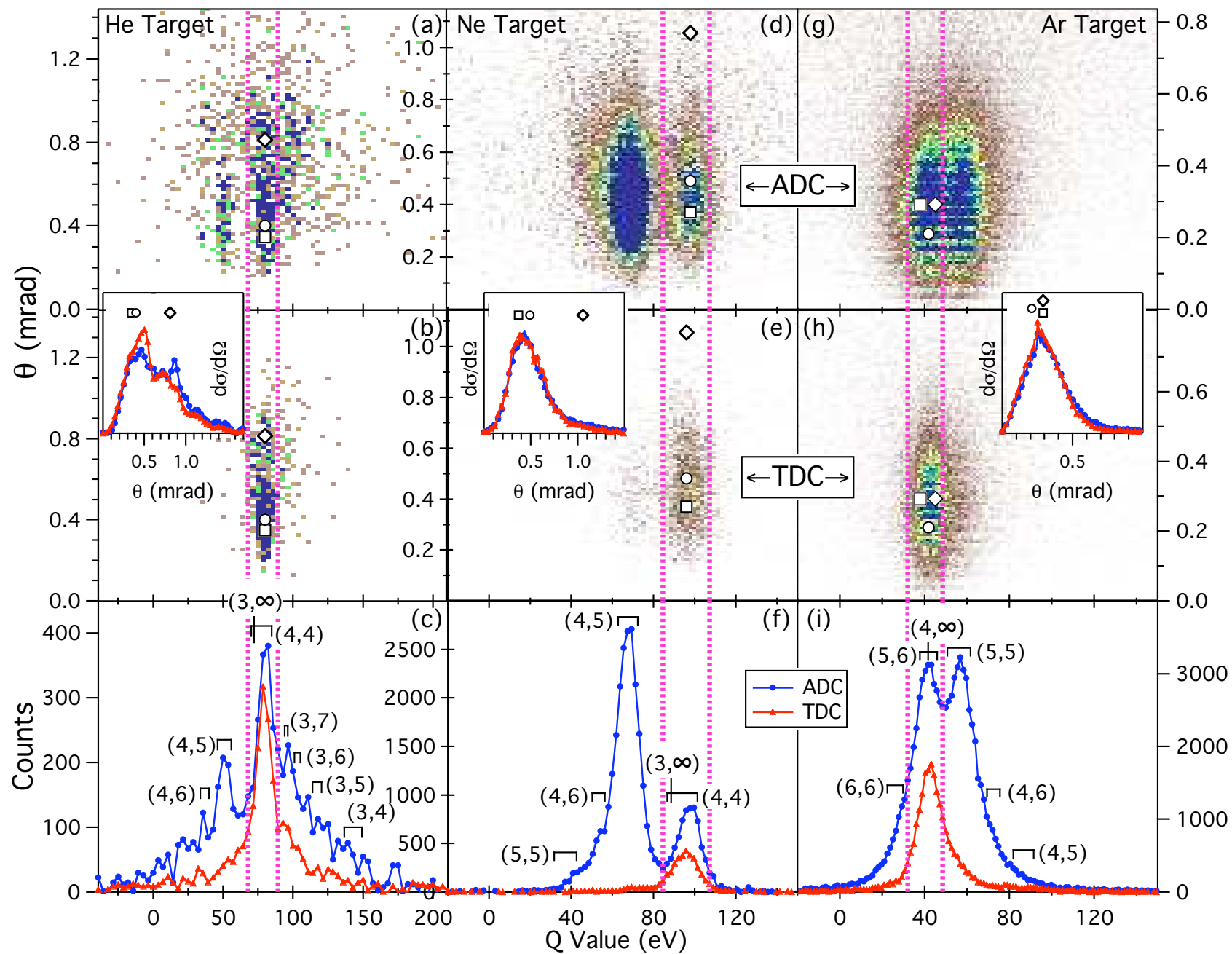


Figure 1

30Dec2015



30Dec2015

Figure 2

